

## A NOVEL THERMAL CRITERION FOR BUBBLE DESTRUCTION IN HYDRODYNAMIC CAVITATION: NUMERICAL MODELING AND EXPERIMENTAL VALIDATION

Anatoliy PAVLENKO\*

*Kielce University of Technology, Aleja Tysiąclecia Państwa Polskiego, 7, 25-314 Kielce, Poland*

Received 12 January 2026; revised 7 February 2026; accepted 10 February 2026

**Abstract.** This research investigates the conditions precipitating the surface instability of spherical bubbles and develops a novel thermal criterion for their terminal collapse during hydrodynamic cavitation. A new mathematical model of vapour bubble dynamics was formulated and implemented in numerical simulations, accounting for heat and mass transfer processes at the bubble interface under various flow conditions. The central hypothesis of the model posits that bubble collapse is triggered when the surface temperature exceeds a critical threshold. Theoretical findings were validated through comparison with experimental data acquired via Venturi tube measurements.

**Keywords:** steam cavitation, bubble dynamics, bubble collapse, mathematical model, numerical simulation, surface instability, hydrodynamic cavitation, heat transfer.

### 1. Introduction

Historically, cavitation has been predominantly examined within the framework of hydrodynamics, focusing on the identification and mitigation of the deleterious effects of erosion on propeller surfaces, hydraulic turbine blades, and various civil engineering structures (Stringer et al., 2023; Kumar et al., 2019; Alcántara Avila et al., 2021; Gawande et al., 2026). Such surface degradation is driven by shock waves and micro-jets generated during the collapse of bubbles, which are traditionally conceptualised as hollow cavities. However, these purely hydrodynamic mechanisms prove insufficient to elucidate the fragmentation of molecular and colloidal structures, the initiation of chemical synthesis, or other micro-scale cavitation phenomena.

A purely hydrodynamic treatment of cavitation precludes the influence of thermal factors on both the development and the distinct manifestations of cavitation effects. To a certain extent, this paradigm persists to the present day; however, it is well-established that during the stage of peak compression, the temperature of the vapour-gas medium within the cavitation bubble exceeds 5.000 K, with pressures escalating to 1.000 MPa (Pavlenko, 2024). It is further postulated (Pavlenko & Koshlak, 2024) that the thermal energy liberated within the bubble volume is sufficient to induce the excitation, ionisation, and dissociation of water vapour molecules

and resident gases. This facilitates the formation of free radicals, enhances gas-phase chemical reaction kinetics by five to six orders of magnitude (Wang et al., 2021; Zhang et al., 2024; Tian et al., 2022), and may even provide the conditions requisite for initiating nuclear fusion within the collapsing cavities (Pan et al., 2024).

Nevertheless, high-temperature processes occurring within the gas phase do not sufficiently elucidate the impact of cavitation on molecular and cellular structures situated in the liquid phase of biological systems. This discrepancy suggests the presence of alternative mechanisms. A rigorous theoretical analysis of cavitation mechanisms is currently constrained by the absence of comprehensive mathematical models that integrate all primary physical factors. Modelling efforts are typically confined to specific experimental scenarios, often neglecting interfacial heat exchange and phase transition kinetics, while frequently assuming adiabatic bubble compression. Autors (Pavlenko & Koshlak, 2021) delineated the thermodynamic principles for a mathematical model of bubble and ensemble dynamics in boiling and cavitation, incorporating key governing factors. The validation of this model against a diverse range of experimental data has demonstrated the efficacy and robustness of this approach.

The objective of the present study is to investigate the mechanisms of cavitation impact on aqueous suspensions containing micro-dispersions, alongside molecular

\* Corresponding author. E-mail: [apavlenko@tu.kielce.pl](mailto:apavlenko@tu.kielce.pl)

and colloidal structures. This investigation is conducted with a view to enhancing the design of cavitating apparatus and establishing optimal operational parameters.

## 2. A modified cavitation model

Notwithstanding the diverse and often conflicting definitions of cavitation, this study adheres to the following general formulation. Cavitation is defined as the complex of phenomena occurring within a liquid when the ambient pressure  $p_{out}$  drops below the saturation vapour pressure  $p_{sat}$  at a given temperature, subsequently followed by a rapid escalation above this threshold. If  $p_{out} < p_{sat}$  the nucleation and growth of vapour bubbles are initiated. Conversely, when  $p_{out} > p_{sat}$  the compression and subsequent terminal collapse of the formed bubbles occur. In both instances, non-equilibrium relaxation processes take place as the bubble system transitions towards a state of thermodynamic equilibrium. This perspective allows both nucleate boiling and cavitation to be described within a unified mathematical framework, utilising the same governing equations albeit under different initial conditions. This conceptual foundation underpins the mathematical model of bubble dynamics presented in (Pavlenko, 2020).

In hydraulic turbines, pumps, and various flow-control devices where the aforementioned pressure gradient conditions are met, the emergence of a pulsating cavitation cluster is inevitable. The periodicity of bubble collapse, the magnitude of pressure and temperature impulses, and the intensity of the spherical shock waves radiated by the cluster are intrinsically dependent upon the flow velocity and the channel geometry within the cavitating zone. These phenomena provide the fundamental principles for the design of diverse cavitating apparatus; notably, in such instances, the initiation of cavitation effects does not necessitate supplementary energy expenditure.

Consider the compression of a vapour bubble in water under the condition  $p_{out} > p_{sat}$ . At the onset of compression, the vapour pressure within the bubble is  $p_v \approx p_{sat}$ , while the pressure in the liquid at the bubble wall,  $p_w$ , is governed by the relation  $p_w = p_v - 2\sigma/R - \mu v_w/R$ . Here,  $R$  denotes the bubble radius,  $v_w$  represents the radial velocity of the liquid at the interface, and  $\sigma$  and  $\mu$  are the coefficients of surface tension and viscosity, respectively. Driven by the pressure differential  $p_{out} - p_v$ , the liquid accelerates towards the bubble centre, resulting in a precipitous increase in both vapour pressure and temperature within the contracting cavity.

The compression rate is governed by interfacial heat transfer and vapour condensation at the cool bubble wall, a process accompanied by the release of latent heat of condensation. Once the internal vapour pressure  $p_v$  exceeds the ambient pressure  $p_{out}$ , the liquid begins to decelerate, and its kinetic energy is converted into the potential energy of the compressed vapour and the

surrounding liquid. Upon the total transformation of this kinetic energy, the compression phase terminates, and the liquid pressure at the bubble interface reaches its peak value. This culminates in a water hammer effect within the vicinity of the bubble, triggering a compression wave that propagates into the bulk liquid at the speed of sound, with its magnitude attenuating as a function of distance.

Conventionally, in the modelling of cavitation processes, the liquid is assumed to be incompressible, thereby neglecting the water hammer effect. To evaluate the significance of this phenomenon, the model previously developed by (Pavlenko & Szwaba, 2025) has been modified to account for liquid compressibility. As part of this enhancement, two new parameters are incorporated into the framework: the liquid compressibility coefficient  $\zeta = f(T, p)$  and the adiabatic compression thermal coefficient  $\Omega(T, p) = \partial T / \partial p$ . By accounting for compressibility, the equation of motion within the model's core system of equations is reformulated as follows:

$$\frac{dv_w}{d\tau} = \frac{\Delta p + 1.6(\Delta p)^2 \zeta - 1.6\rho v_w^2}{\rho R}, \quad (1)$$

where  $\Delta p = p_w - p_{out}$  and  $\rho$  denotes the liquid density. In contrast to the classical Rayleigh–Plesset equation, which is conventionally employed to describe cavitation processes in incompressible fluids, Equation (1) is distinguished by the presence  $1.6(\Delta p)^2 \zeta$  in the numerator. This term accounts for the contribution of the potential energy of the compressed liquid, which is subsequently manifested as an acoustic pulse. The speed of sound within the liquid is determined by the relation  $c^2 = (\rho\zeta)^{-1}$ . Following the transition of the vapour parameters into the supercritical regime within the compressed bubble, the liquid–vapour interface vanishes. In place of the bubble, a quasi-spherical high-temperature “thermal” is formed, within which water undergoes a continuous transition from a supercritical state to a condensed phase (Pavlenko, 2020). The radius of the region, characterised by a central pressure  $p_{max}$  and a peripheral pressure  $p_{cr}$  at its external boundary, is estimated using the relation

$$R_{cr} = R \sqrt{\frac{p_{max}}{p_{cr}}},$$

while its duration is determined by the formula  $\tau_{cr} = 2R_{cr}/c$ . The values of  $R$  and  $p_{max}$  are derived within the model during the computational procedure, contingent upon the respective initial conditions. Contained within this supercritical pressure region is a spherical zone, where the temperature reaches  $T_{max} > T_{cr}$  at its centre and declines to  $T_{cr}$  at its outer boundary. The existence of this high-temperature zone is attributed to heat transfer from the vapour to the liquid phase, the release of latent heat of condensation, and the heating of the liquid during shock compression. Within this region, water exists in a supercritical fluid state. Computational results indicate that while the residence time of water in

the supercritical fluid state does not exceed 10 ns, this represents an exceedingly significant duration, given that the characteristic timescales for most chemical reactions and the formation of molecular structures are measured on a picosecond scale.

### 3. Numerical modelling of cavitation dynamics

Figure 1 illustrates the experimental distribution (Koshlak & Pavlenko, 2025; Soyama et al., 2023) of static pressure along the channel,  $p = f(x)$ , alongside the variation in the surface temperature,  $T = f(x)$  of a cavitation bubble traversing the nozzle with the flow. The temperature exceeds the critical threshold  $T_{cr}$  within the divergent section of the nozzle; according to experimental data, this leads to the disintegration of the bubble specifically within this region. The dissipated power is expended on the localised evaporation of the liquid and the subsequent formation of a vapour cavity. Due to inertia, the resulting vapour bubbles expand to a maximum radius  $R_{max}$ . At this peak dimension, the internal vapour pressure is significantly lower than the ambient liquid pressure, thereby facilitating rapid bubble contraction. As previously highlighted, the modelling of such bubble dynamics is hindered by significant challenges, primarily due to the fact that the internal vapour pressure and temperature at the maximum radius  $R = R_{max}$  are beyond the reach of direct experimental measurement. Consequently, the precise initial conditions required to characterise the onset of bubble collapse remain indeterminate.

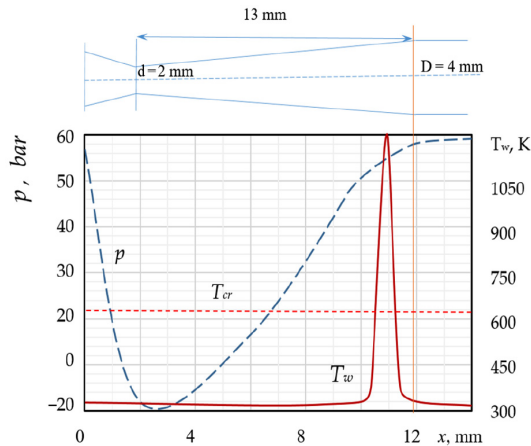


Figure 1. Analysis of experimental data (Koshlak & Pavlenko, 2025) regarding cavitation bubble collapse within a water flow inside a Venturi nozzle, induced by static pressure variations along the channel length

Figure 2 illustrates the evolution of internal vapour pressure within an oscillating bubble according to the proposed modified model.

The bubble disintegrates after three to four oscillations, once the temperature exceeds the critical threshold,  $T_{cr}$ . As illustrated in Figure 2, the peak vapour temperatures within the bubble during the maximum

compression phase increase with each successive oscillation cycle. In the present case, the temperature surpasses the critical value only during the fourth period of oscillation, leading to the irreversible disintegration of the bubble. These findings are in qualitative agreement with the results observed in steam cavitation experiments (Koshlak & Pavlenko, 2025; Soyama et al., 2023).

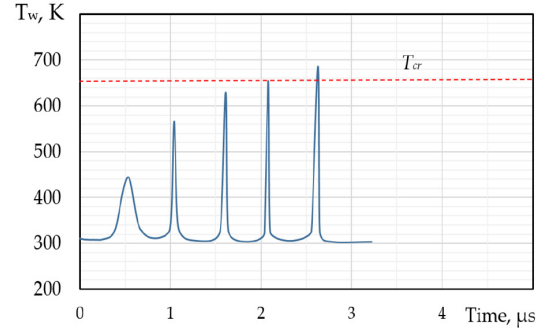


Figure 2. Temperature evolution within a vapour bubble during collapse. Calculations are based on the experimental conditions (Koshlak & Pavlenko, 2025):  $T = 293$  K,  $p = 1$  bar;  $R = 10$   $\mu$ m

As the degree of liquid subcooling  $\Delta T$  increases, the peak temperatures rise accordingly. Under conditions of high subcooling ( $\Delta T > 48$  K), the temperature during the maximum compression phase exceeds  $T_{cr}$  as early as the second to fourth oscillation cycle. This triggers bubble disintegration due to the thermal instability of the interface. Conversely, at lower values of  $\Delta T$ , the condition  $T > T_{cr}$  is never satisfied in any oscillation period; consequently, the bubble undergoes damped oscillations until the vapour is fully condensed. Calculations indicate that the thermal boundary between these two collapse regimes corresponds to a water temperature of 325 K (a subcooling degree of  $\Delta T = 48$  °C). The existence of sustained bubble oscillations without disintegration in slightly subcooled liquids is corroborated by experimental data (Koshlak & Pavlenko, 2025). This analysis provides a basis for asserting that the mechanism of interfacial thermal instability may explain the spontaneous disintegration of relatively large bubbles in steam cavitation processes.

### 4. Influence of operating parameters on bubble dynamics

Using a modified numerical model, the influence of liquid temperature and pressure on cluster dynamics was evaluated under the experimental conditions (Koshlak & Pavlenko, 2025; Soyama et al., 2023). Furthermore, the kinetics of energy and mass transfer across the phase interface during bubble oscillation were analysed. The results of the computational experiment are presented below. Among all operational parameters, liquid temperature was found to exert the most significant influence

on bubble dynamics during vapour cavitation. Variations in temperature qualitatively alter the nature of bubble oscillations during the collapse phase. A sharp reduction in the amplitudes of kinematic and dynamic parameters, including velocity ( $v_w$ ), acceleration ( $dv_w/d\tau$ ), and internal vapour temperature and pressure, is observed with increasing  $T$ . Additionally, the amplitude of radial size pulsations is substantially diminished. Figure 3 illustrates the dependence of the bubble radius on liquid temperature within the range of 20 to 80 °C. The dashed portion of the plot characterises a bubble state that is likely physically unattainable, as the cavitation bubble would typically fragment prior to reaching this point. Whilst bubble collapse is accompanied by intense radial oscillations at relatively low temperatures, the bubble collapses almost monotonically, exhibiting only weak pulsations, in more heated liquids.

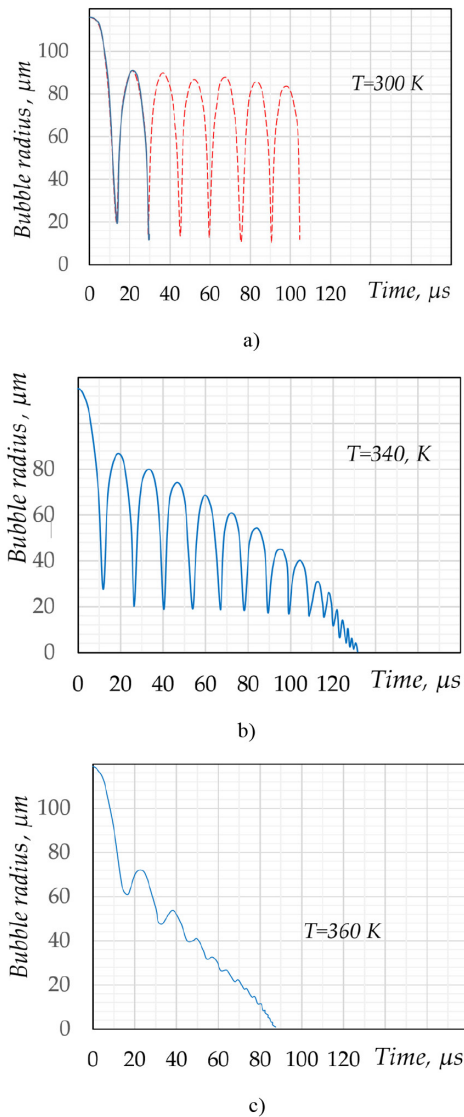


Figure 3. Temporal evolution of the vapour bubble radius during the collapse phase in a subcooled liquid as a function of liquid temperature. Numerical results correspond to the experimental conditions reported by Koshlak and Pavlenko (2025); water temperature: a – 300 K; b – 340 K; c – 360 K

The extent to which temperature variations influence the kinematic and dynamic parameters of the liquid in the vicinity of the bubble is demonstrated in Figure 4. This figure illustrates the dependence of the peak radial velocity and specific power at the bubble interface on the degree of liquid subcooling. As the liquid temperature increases from 20 to 90 °C, the peak velocity values decrease by three to four orders of magnitude, while the specific power diminishes by nine to ten orders of magnitude.

A similarly pronounced temperature dependence is observed for the amplitudes of the pressure pulses emitted by bubbles collapsing in the subcooled liquid. For all three relationships depicted in the figure, a disruption of monotonicity is observed within the temperature interval of  $\Delta T = 45\text{--}50$  °C. Specifically, the specific power undergoes a nearly step-wise change of one order of magnitude in this region. This non-monotonic behaviour was also recorded for the peak values of other parameters, including vapour pressure and temperature, mass flux, and specific heat.

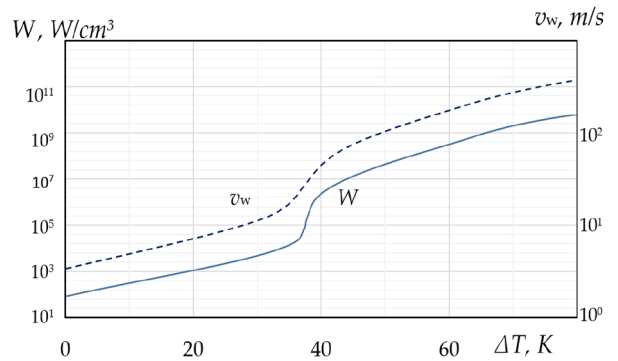


Figure 4. Dependence of the peak radial expansion velocity and specific power in the bubble vicinity at the instant of maximum compression on the degree of water subcooling

The pronounced influence of liquid temperature on bubble dynamics offers a potential pathway for regulating the intensity of the dynamic impact exerted by cavitation clusters induced by vapour cavitation. In this study, the effect of ambient liquid pressure within the cavitator on the behaviour of vapour bubbles in subcooled liquids was investigated across a pressure range from 0.02 MPa to 0.5 MPa. Calculations were performed at constant temperature values. It was assumed that  $T_{\text{boil}} = f(p)$ , and the temperatures of the water and vapour were selected to ensure that the liquid remained subcooled while the vapour was superheated relative to the saturation temperature  $T_{\text{boil}} = f(p)$  throughout the investigated pressure range. Figure 5 illustrates the dependence of the peak vapour pressure pulse  $p_v$  and the specific power  $W$  at the bubble interface on the ambient liquid pressure. A pressure maximum is observed in the region of 0.1 MPa, which may, at first glance, appear counter-intuitive. The reduction in the dynamic characteristics of the bubble at lower pressures is expected, as it stems from a decrease

in the pressure differential,  $p_{\text{out}} - p_{\text{sat}}(T)$ , which governs the intensity of the collapse.

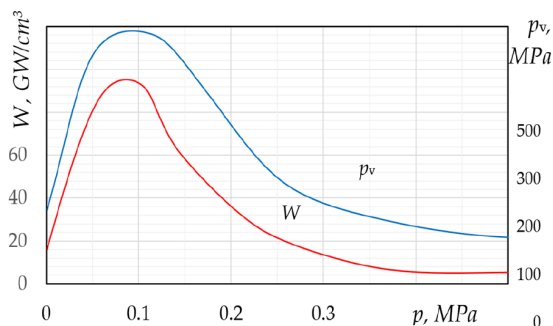


Figure 5. Dependence of the specific power in the bubble vicinity and the internal vapour pressure on the ambient liquid pressure  $p_v$

As the external static pressure increases ( $p > 0.1$  MPa), the initial pressure differential,  $p_{\text{out}} - p_{\text{sat}}(T)$ , rises. Theoretically, this should facilitate an increased rate of vapour condensation and lead to a more intense collapse, accompanied by the emission of high-magnitude pressure pulses. However, this factor appears to be counterbalanced by a reduction in the collapse velocity, which results from the higher initial vapour content within the bubble. The existing literature lacks experimental data regarding bubble cavitation in subcooled liquids across varying static pressures. Nevertheless, an extensive body of information exists regarding acoustic cavitation at various static pressures, confirming the presence of a maximum in the relationship between cavitation intensity and pressure. This characteristic enables the selection of optimal operational regimes when employing acoustic cavitation to intensify processes such as dispersion and emulsification. It is generally (Xu et al., 2024; Apte et al., 2024) maintained that the collapse velocity of a single bubble should increase monotonically with rising static pressure. The attenuation of dynamic cavitation effects at high pressures is typically attributed to the reduction in the population of cavitation bubbles as external pressure increases; in our view, this decrease in bubble count compensates for the intensified dynamics of individual bubbles.

## 5. Conclusions

The study of hydrodynamic cavitation, with a view to its targeted and efficient application for the stimulation and intensification of chemical engineering processes in nano- and biotechnology, necessitates a unified approach that equally accounts for both the hydrodynamic and heat-and-mass transfer aspects of the phenomenon. Within this framework, a mathematical model is being developed and refined to adequately describe the behaviour of individual bubbles and bubble ensembles in boiling and cavitation processes, incorporating all governing

factors and precise thermophysical system parameters. The findings of this research demonstrate that when analysing cavitation effects on supramolecular and microbiological entities, as well as on chemical reaction kinetics, it is essential to consider the phase transition of both the liquid surrounding the bubble and the vapour-gas mixture within it into a supercritical fluid state. To evaluate the spatio-temporal boundaries of the supercritical region and to analyse spherical water hammer effects within localised zones of the cavitation cloud, liquid compressibility must be incorporated into the modelling. This study should be regarded as a foundational step towards establishing rational designs and optimal operating regimes for cavitating devices across various technological applications.

## References

- Alcántara Avila, J. R., Kong, Z. Y., Lee, H.-Y., & Sunarso, J. (2021). Advancements in optimization and control techniques for intensifying processes. *Processes*, 9, Article 2150. <https://doi.org/10.3390/pr9122150>
- Apte, D., Ge, M., Zhang, G., & Coutier-Delgosha, O. (2024). Numerical investigation of three-dimensional effects of hydrodynamic cavitation in a Venturi tube. *Ultrasonics Sonochemistry*, 111, Article 107122. <https://doi.org/10.1016/j.ultsonch.2024.107122>
- Gawande, G., Mali, P., Dhavane, P., & Nahata, Y. (2026). Hydrodynamic cavitation – A promising technology for water treatment. *Materials Today: Proceedings*, 124, 129–139. <https://doi.org/10.1016/j.matpr.2024.05.075>
- Koshlak, H., & Pavlenko, A. (2025). A new mathematical model for the features of bubble collapse in steam. *Cavitation processes*, 15(18), Article 9948. <https://doi.org/10.3390/app15189948>
- Kumar, C., Hejazian, M., From, C., Saha, S. C., Sauret, E., Gu, Y., & Nguyen, N.-T. (2019). Modeling of mass transfer enhancement in a magnetofluidic micromixer. *Physics of Fluids*, 31, Article 063603. <https://doi.org/10.1063/1.5093498>
- Pan, X., He, L., Tian, Z., Zhang, R., Hua, M., Fang, Y., & Ji-ang, J. (2024). Experimental research on the explosion boiling mechanism of superheated liquids containing short chain alcohol impurities with different boiling points. *Applied Thermal Engineering*, 238, Article 121998. <https://doi.org/10.1016/j.applthermaleng.2023.121998>
- Pavlenko, A. (2020). Energy conversion in heat and mass transfer processes in boiling emulsions. *Thermal Science and Engineering Progress*, 15, Article 100439. <https://doi.org/10.1016/j.tsep.2019.100439>
- Pavlenko, A. (2024). Numerical modeling of the behavior of bubble clusters in cavitation processes. *Energies*, 17(7), Article 1741. <https://doi.org/10.3390/en17071741>
- Pavlenko, A. M., & Koshlak, H. (2021). Application of thermal and cavitation effects for heat and mass transfer process intensification in multicomponent liquid media. *Energies*, 14, Article 7996. <https://doi.org/10.3390/en14237996>
- Pavlenko, A., & Koshlak, H. (2024). Study of the dynamics of a single bubble. *Energies*, 17, Article 4236. <https://doi.org/10.3390/en17174236>

- Pavlenko A., & Szwaba, R. (2025). Behaviour of vapour bubbles in an acoustic field. *Applied Thermal Engineering*, 280(Part 4), Article 128495. <https://doi.org/10.1016/j.applthermaleng.2025.128495>
- Soyama, H., Liang, X., Yashiro, W., Kajiwara, K., Asimakopoulou, E. M., Bellucci, V., Birnsteinova, S., Giovanetti, G., Kim, C., Kirkwood, H. J., Koliyadu, J. C., Letrun, R., Zhang, Y., Uličný, J., Bean, R., Mancuso, A. P., Villanueva-Perez, P., Sato, T., Vagovič, P., Eakins, D., & Korsunsky, A. M. (2023). Revealing the origins of vortex cavitation in a Venturi tube by high speed X-ray imaging. *Ultrasonics Sonochemistry*, 101, Article 106715. <https://doi.org/10.1016/j.ultsonch.2023.106715>
- Stringer, M., Zeng, Z., Zhang, X., Chai, Y., Li, W., Zhang, J., Ong, H., Liang, D., Dong, J., Li, Y., Fu, Y., & Yanget, X. (2023). Methodologies, technologies, and strategies for acoustic streaming-based acoustofluidics. *Applied Physics Reviews*, 10, Article 011315. <https://doi.org/10.1063/5.0134646>
- Tian, Z., Shang, Q., Pan, X., Zhang, R., Hua, M., Zhao, Y. & Jiang, J. (2022). Experimental study on explosive boiling mechanism of superheated liquid containing ethanol impurities under rapid depressurization. *Process Safety and Environmental Protection*, 168, 443–453. <https://doi.org/10.1016/j.psep.2022.09.073>
- Xu, Y., Liu, H., Wang, Z., Zhang, J., & Wang, J. (2024). Analysis of the effects of nozzle geometry on the cavitation water jet flow field using orthogonal decomposition. *Iranian Journal of Science and Technology, Transactions of Mechanical Engineering*, 48, 119–132. <https://doi.org/10.1007/s40997-023-00647-9>
- Wang, B., Su, H., & Zhang, B. (2021). Hydrodynamic cavitation as a promising route for wastewater treatment – A review. *Chemical Engineering Journal*, 412, Article 128685. <https://doi.org/10.1016/j.cej.2021.128685>
- Zhang, K., Zheng, J., Xu, Y., Liao, Z., Huang, Y. & Lu, L. (2024). Enhanced fabrication of size-controllable chitosan-genipin nanoparticles using orifice-induced hydrodynamic cavitation: Process optimization and performance evaluation. *Ultrasonics Sonochemistry*, 106, Article 106899. <https://doi.org/10.1016/j.ultsonch.2024.106899>